Technical Report **R 214**

THE TWO CURRENT-PROBE METHOD OF MEASURING CONDUCTED RADIO-FREQUENCY INTERFERENCE

28 September 1962

U. S. NAVAL CIVIL ENGINEERING LABORATORY

Port Hueneme, California

THE TWO CURRENT-PROBE METHOD OF MEASURING CONDUCTED RADIO-FREQUENCY INTERFERENCE

Y-F006-09-205

Type B

by

James L. Brooks

ABSTRACT

A new approach to the problem of measuring conducted interference is described. A brief discussion is presented on the limitations and uncertainties of the presently accepted method using Line-Impedance-Stabilization Networks (LISN). These limitations stem from the fact that no information is obtained concerning the impedance values of the circuit being measured during a noise measurement. The new method described provides a means of overcoming the limitations of the present method completely by the use of commercially available current-probes in an impedance- and noise-measurement system.

A method of determining the impedance values of the circuit has been worked out which requires the use of two current-probes. Either the noise-source impedance or the load impedance or both may be determined by this method. Two separate measurements and calculations are required however, one to determine the magnitude of the impedance and the other to determine the phase angle.

An evaluation of the device is presented, as well as numerous examples of noise measurements showing the correlation between measured and predicted results.

The precision of the impedance-measuring system is within 20 percent throughout the frequency range of 2 to 30 megacycles where phase angle is measured for most of the commonly encountered line and source impedance values. For measurement of impedance magnitudes, the accuracy of the system is better than 20 percent for the range of the current-probes (100 kilocycles to 100 megacycles).

INTRODUCTION

The project is concerned with providing a better method for performing RFI acceptance tests on equipment such as electric motors, transmitters, etc., procured by the Bureau. The present method as set forth by Mil-I-16910A using line-impedance-stabilization networks leaves considerable doubt as to the true value of the conducted RFI existing on the power connections of the equipment tested.

Since electrical noise may be narrow band or broadband in nature, and may be either radiated or conducted from the source, the instruments used to monitor the noise-voltage levels are highly sensitive frequency-selective devices with output meters calibrated in microvolts across a specified input impedance of 50 ohms. It is mandatory that the input impedance remain constant in order to maintain good calibration over the frequency band of the instrument.

Unfortunately, when used as a two-terminal voltmeter in the LISN measurement, the low impedance of the meter presents considerable loading to circuits of higher impedance levels. A high-impedance blocking network such as the line-impedance-stabilization network is presently used to isolate the device under test from its power connection and provide a known load across the line.

PROBLEM ANALYSIS

Given: An electrical or electronic device which is to be tested for conducted radio interference to determine its acceptability.

Figure 1 shows the schematic. It is the purpose of this test to determine the noise voltage ($\bar{V}_n$).

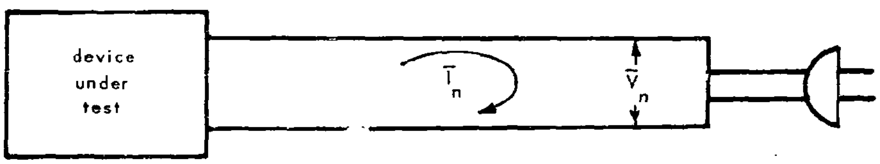

Figure 1. Electrical noise and current on power cord.

The device under test may be replaced by an equivalent noise source and impedance (Figure 2).

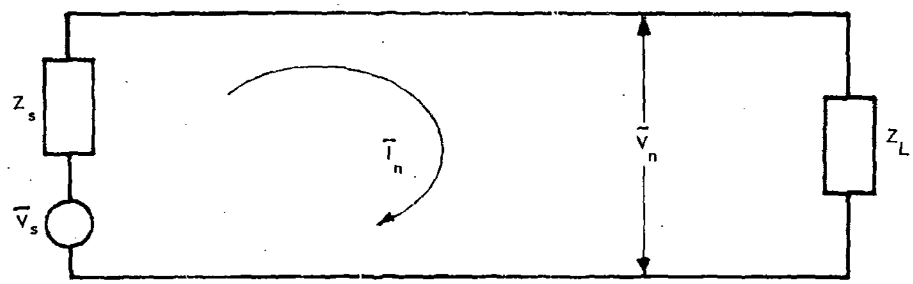

Figure 2. RF equivalent circuit of device under test.

where $\bar{V}_s$ = equivalent noise-source voltage

Z_s = equivalent noise-source impedance

$\bar{I}_n$ = noise current on the power cord

$\bar{V}_n$ = noise voltage across the power cord at point of measurement

Z_L = equivalent load impedance of the power outlet

The circuit equations are:

$$\bar{V}_s = \bar{I}_n Z_s + \bar{V}_n \tag{1}$$

$$\bar{V}_n = \bar{I}_n Z_L \tag{2}$$

$$\bar{V}_n = \bar{V}_s \left(\frac{1}{1 + \frac{Z_s}{Z_L}} \right) \tag{3}$$

PRESENT METHOD

It is apparent that connecting the RFI meter across the line as a two-terminal voltmeter would load the circuit and yield unreliable readings, particularly when the source impedance and load impedances are greater than 50 ohms. For this reason a different approach has been taken.

The usual method for making conducted interference measurements is to insert a network into the line which will effectively block out the load impedance and provide a known impedance for the noise source to work into. These networks have been designed, are available commercially, and are called line-impedance-stabilization networks. The circuit diagram of a typical line-impedance-stabilization network is shown in Figure 3.

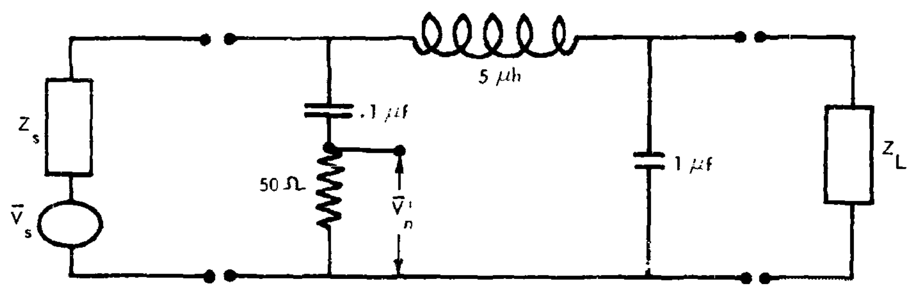

Figure 3. Line-impedance-stabilization network.

The noise voltage (V_n') measured with the noise meter in this circuit is of course not the voltage that would appear on the line with the network removed, due to the loading effect of this network on the device under test. As a matter of fact, the voltage measured in this manner gives no indication at all as to what voltage would actually appear on the line with the network removed since the noise-source impedance and the load impedance are normally not known. The best that can be done with this LISN is to say that the voltage measured is at least repeatable for identical hookups and to record the readings as induced voltages into the LISN. The equivalent circuit using the LISN is similar to that for the normal situation, as shown in Figure 2, with the exception of the load impedance, which is now 50 ohms (see Figure 4).

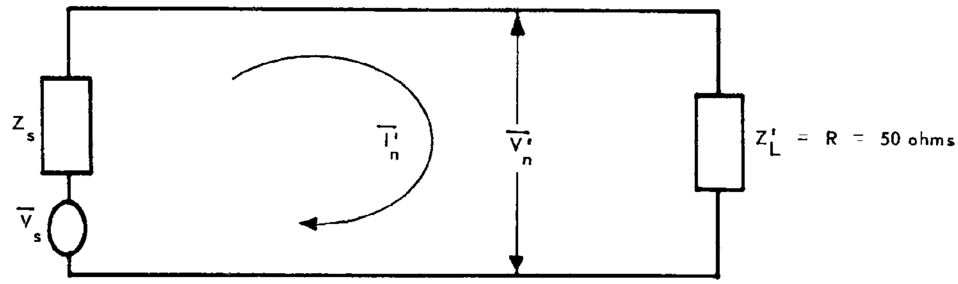

Figure 4. RF equivalent circuit with LISN inserted.

The circuit equation for this situation is:

$$\overline{V}'_n = \overline{V}_s \left(\frac{1}{1 + \frac{Z_s}{R}} \right) \tag{4}$$

It is obvious that unless the normal load impedance Z_L happens to be 50 ohms the voltage reading across the LISN will not be the correct voltage existing on the line in the normal situation. The voltage difference may be represented vectorily as shown in Figure 5.

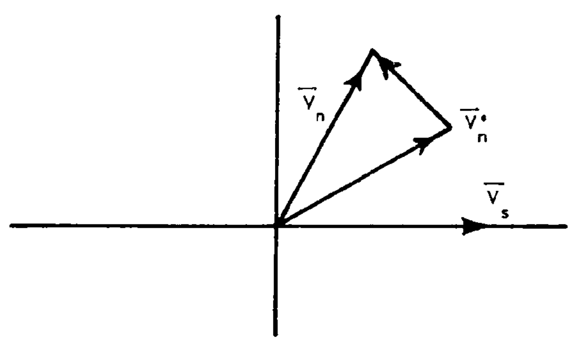

Figure 5. Vector diagram showing the difference between the normal noise voltage ($\overline{V}_n$) and the noise voltage measured using a LISN ($\overline{V}'_n$).

The vector difference $\overline{V}_n - \overline{V}_n'$ is clearly a function of the impedances of the circuit and will henceforth be called the error voltage. An investigation into the possible range of the error voltage is now in order.

The quantities Z_s and Z_L are both physical impedances and as such may range in magnitude from 0 to ∞ and from -90 to +90 degrees in phase angle. Therefore the quantity Z_s/Z_L may range from 0 to ∞ in magnitude and from -180 to +180 degrees in phase angle. Also the quantity Z_s/R may range from 0 to ∞ in magnitude but only from -90 to +90 degrees in phase angle.

It immediately becomes apparent that the term $1/[1 + (Z_s/Z_L)]$ which appears in Equation 3 may possess a discontinuity when $Z_s/Z_L = -1$; otherwise it is well-bounded. However the quantity $1/[1 + (Z_s/R)]$ from Equation 4 does not possess discontinuities and is well-bounded between 0 and 1.

The equation for the error voltage may be written as:

$$\overline{V}_{err} = \left|\overline{V}_n - \overline{V}_n'\right| = \overline{V}_s \left|\frac{1}{1 + \frac{Z_s}{Z_L}} - \frac{1}{1 + \frac{Z_s}{R}}\right| \qquad (5)$$

As pointed out above, the first term of the error voltage equation possesses a discontinuity at $Z_s/Z_L = -1$ which represents a maximum error situation. Figure 6 shows a plot of the error equation, as derived in Appendix A.

The following significant points to be derived from Figure 6 are:

1. The discontinuity occurs at $Z_s/Z_L = -1$ at 180 degrees.

2. There is only one discontinuity point.

3. The error due to phase angle is only appreciable when $0.1 < Z_s/Z_L < 10$.

4. The error voltage due to differences in magnitude alone of the impedances will not exceed $\overline{V}_s$.

5. The probability of occurrence of the point of discontinuity is extremely small. This point requires a simultaneous occurrence of two independently improbable situations before the error voltage can approach infinity: (a) the impedance-magnitude ratio must be exactly equal to 1; and (b) the phase angle of the ratio must be exactly 180 degrees.

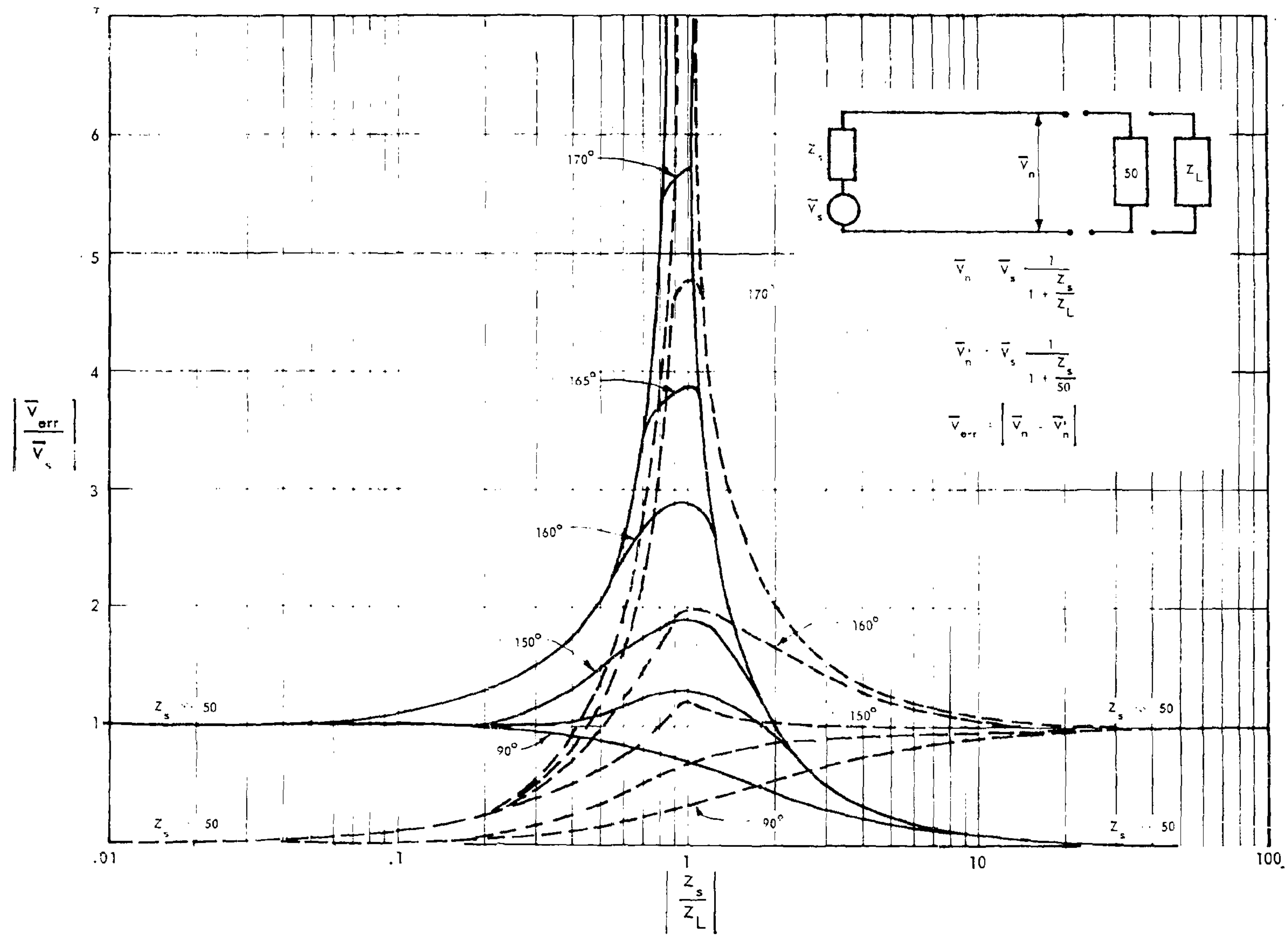

Figure 6. Curves showing the maximum possible error voltage referred to the noise-source voltage as a function of the source impedance referred to the load impedance.

The second requirement for the discontinuity point is even more improbable than the first since it requires impedances which possess infinite Q's, or in other words, pure reactive values. As stated before, the actual impedances possess a certain amount of resistance, which in turn lowers the Q of the circuits, therefore lowering the maximum error voltage. This resonance effect is shown by the family of curves in Figure 6.

For the foregoing reasons, the presently accepted method of measuring conducted interference is unsatisfactory. No information concerning impedance values in the circuit is obtained during a measurement, resulting in considerable inaccuracy of the readings. Hence a different approach to the measurement problem was taken. It is therefore the object of this task to develop a circuit or circuits that can provide a true indication of conducted interference from the variety of electrical items being tested for RFI.

CONTRACT WORK AND REPORT

This Laboratory contracted with the Stoddart Aircraft Radio Corporation, Los Angeles, to investigate the possibilities of using the two current-probe method of measuring conducted RFI and impedance and to build a prototype instrument for this purpose.

The work performed by the contractor is described in detail in his final report.* The high points of that report will be mentioned here.

The contract requirements were:

1. To study and evaluate presently used line-impedance-stabilization networks and new networks now in production or being proposed.

2. To investigate new techniques of measuring conducted interference using the Stoddart current-probe and probes for measurement of interference and RF impedances of noise sources.

3. To make interference and impedance measurements as necessary to obtain supporting data when such data was not otherwise available.

4. If comparison and correlation studies disclosed a need for new techniques, and/or devices for the measurement of conducted interference, recommendations relative thereto should be given to the fullest extent practicable.

* Stoddart Aircraft Radio Co., Inc. Improved Line Impedance Stabilization Method, by J. W. Shaw and E. R. Byerley. Hollywood, Calif., October 1960.

The contractor conducted a literature search into the many phases of conducted-interference-measurement techniques used in the past as well as the presently accepted methods. This search pointed out the following disadvantages of the presently accepted method of measuring conducted interference with LISN networks:

1. The four-terminal impedance-stabilization network must be inserted into the noise-carrying line.

2. This insertion is likely to change the actual noise current flowing in the line because of a concomitant change of circuit parameters.

3. The physical size of the 5-microhenry choke limits the power-current level at which the impedance-stabilization network may be used.

Significant work performed by the Naval Material Laboratory at New York Naval Shipyard, Brooklyn, was described. A dual and single line-impedance-stabilization network were designed, which made it possible to measure conducted radio interference up to 100 megacycles with repeatable results. The dual unit was limited to 5 amps, the single unit to 50 amps.

The contractor proposed a new method for measuring conducted interference; however the analysis presented in the contract report is incomplete and difficult to follow. Therefore a simpler approach is presented. This method can best be explained by returning to the noise-source equivalent circuit in Figure 2. A review of the circuit equations shows that the noise voltage $\overline{V}_n$ could be determined easily if $\overline{I}_n$ and Z_L were known. The system to be described here makes it possible to determine these values by utilizing commercially available current-probes.

The assumption is made that even though the quantities $\overline{V}_s$, $\overline{V}_n$, and $\overline{I}_n$ are broadband in nature, when measured with a narrow-bandwidth instrument, they will display c-w (continuous-wave) characteristics and will be treated accordingly. As a direct result of this, the impedances involved will have a bandwidth dependence associated with them; however, they too will be treated as normal c-w impedances. Unless resonances in the impedance characteristics occur, the impedance change within the RFI-meter bandwidth will be small.

The noise current $\overline{I}_n$ may be measured directly, as shown in Figure 7. The current-probe reflects a constant low impedance into the circuit and therefore generally yields accurate readings.

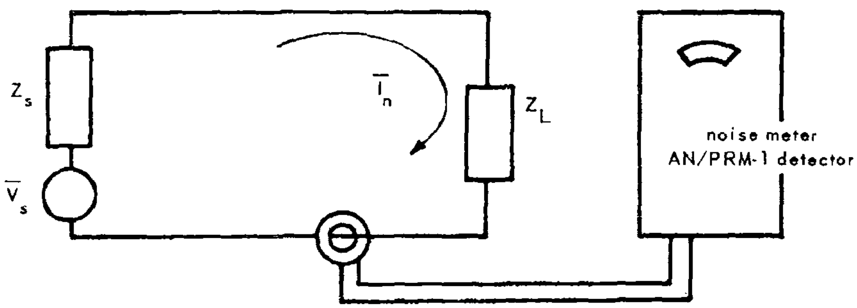

Figure 7. Measurement of noise current $\overline{I}_n$.

The equivalent load impedance Z_L can be measured as shown in Figure 8.

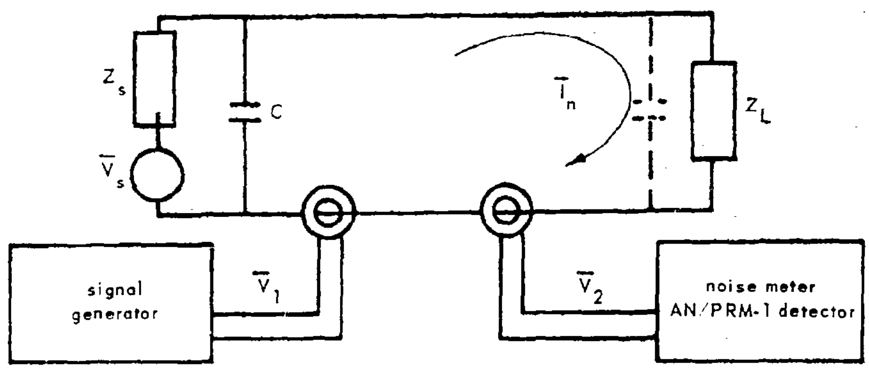

Figure 8. Measurement of load impedance Z_L.

This circuit may be redrawn as shown in Figure 9.

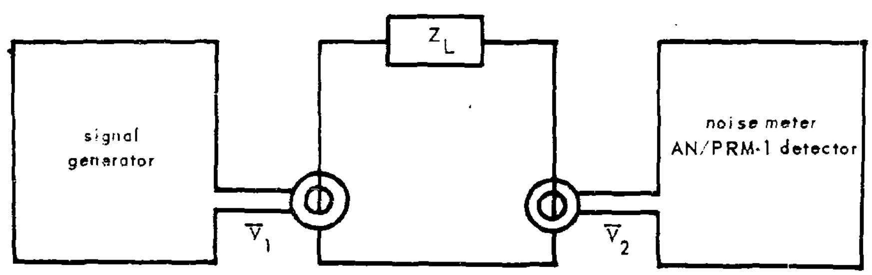

Figure 9. RF equivalent circuit for measuring Z_L.

The equation for the impedance Z_L as derived from this configuration in Appendix B is:

$$\left|Z_L\right| = K \left(\left| \frac{\overline{V}_1}{\overline{V}_2} \right| - 1 \right) \tag{6}$$

where K is the noise-meter impedance reflected into the measuring circuit.

The noise voltage $\overline{V}_n$ existing across the impedance Z_L of the line may now be determined by the equation

$$\left|\overline{V}_n\right| = \overline{I}_n \left|Z_L\right| \tag{7}$$

The noise-source voltage $\overline{V}_s$ may be determined in a similar manner by first moving the shorting capacitor to the dotted-line position (see Figure 8) and measuring $|Z_s|$. Once $|Z_s|$ is determined, $\overline{I}_n$ may be measured for this new situation and $\overline{V}_s$ determined by the relation $\left|\overline{V}_s\right| = \overline{I}_n |Z_s|$.

Based on the above theory, a prototype instrument was built; the features were:

1. The impedance-magnitude-measuring capability is limited by the current-probe transfer impedance which has a 3-db bandwidth of 0.5 to 45 megacycles.

2. The impedance-magnitude-measurement accuracy is within 20 percent when averaged values for K are used in Equation 6, or better than 10 percent when a $\overline{V}_1/\overline{V}_2$ versus frequency nomograph is used in the computations (see Figure 10).

3. The power-current-carrying capability is 350 amps ac or dc.

4. The instrument is constructed entirely of passive circuitry.

5. A photograph of the instrument is shown in Figure 11.

The contractor measured the impedance of various electrical networks and noise sources. An example of one of those tests is shown in Figure 12. In this test a 20-foot length of coaxial cable was shorted on one end by a Type N shorting termination; the other end was used to form a small loop for coupling the probes.

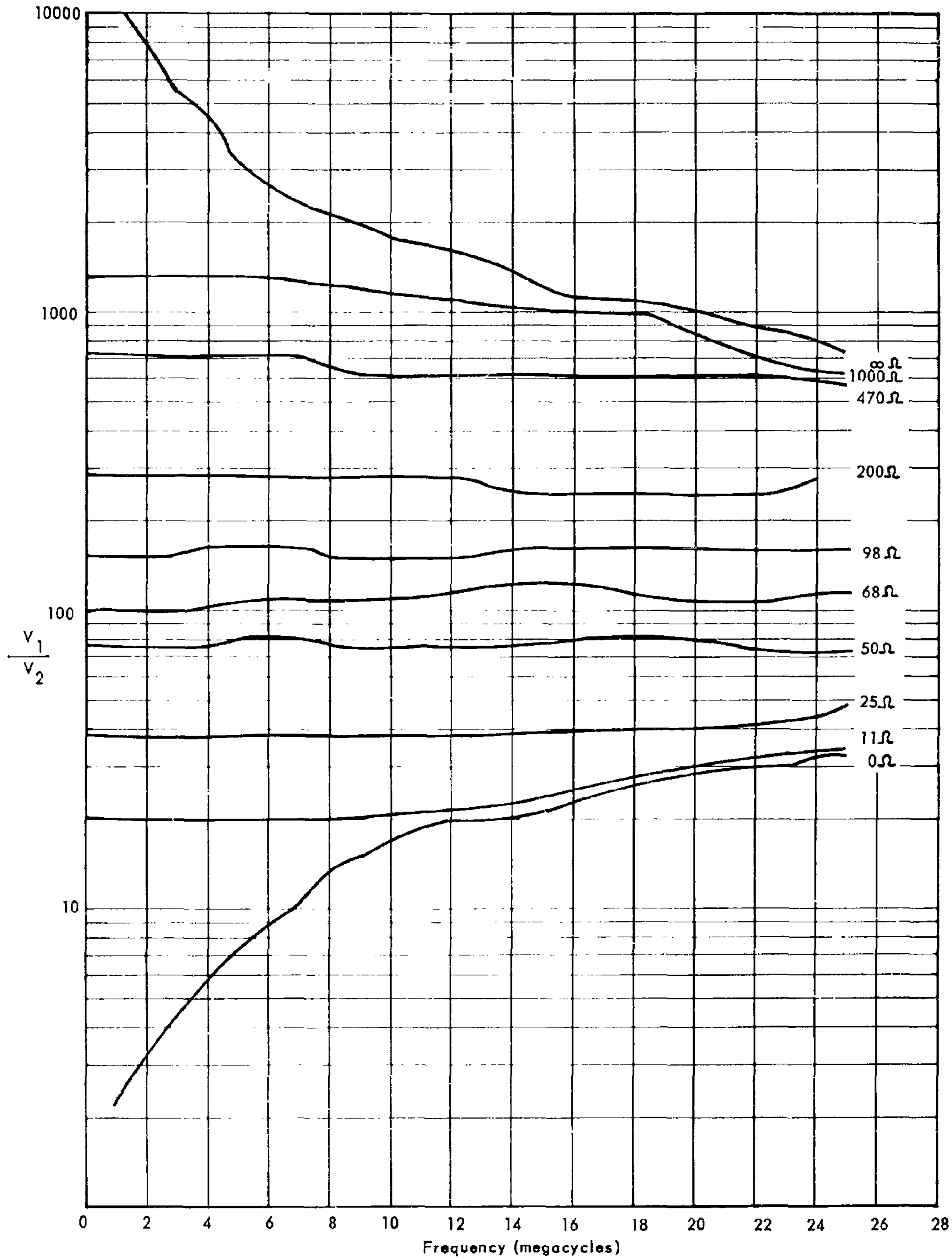

Figure 10. Line-impedance measuring-device impedance versus frequency nomograph.

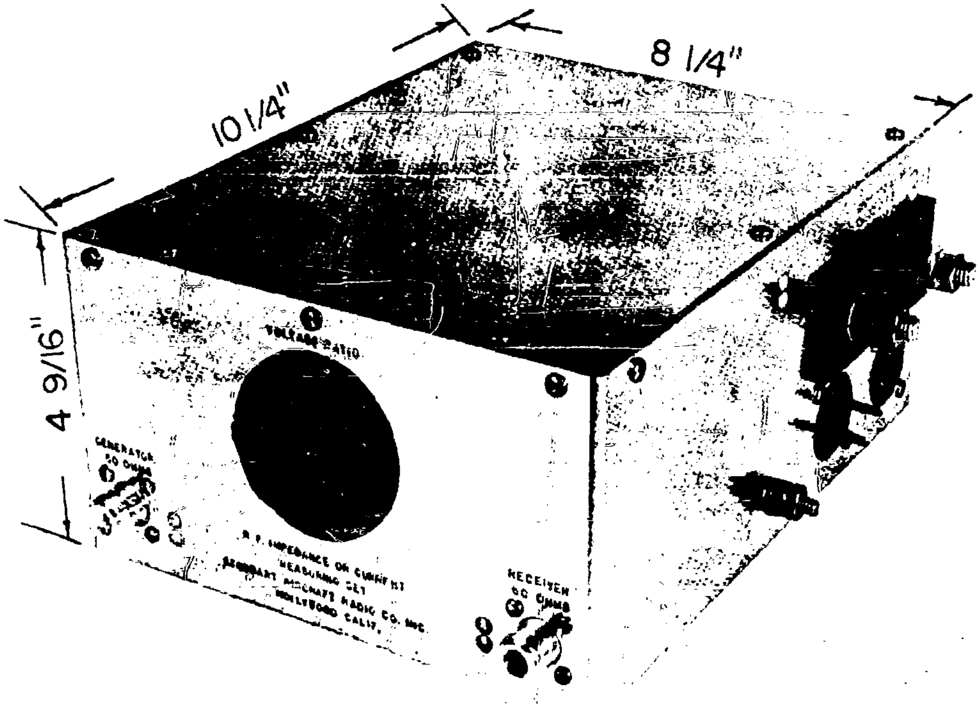

Figure 11. RF impedance- or current-measuring set.

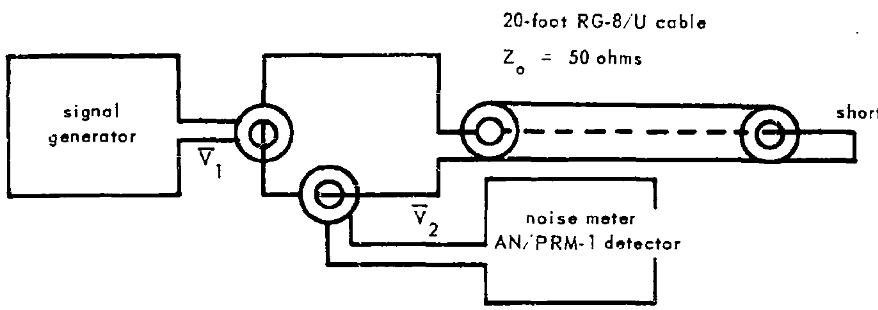

Figure 12. Measurement of RF impedance of 20-foot length of RG-8/U coaxial cable shorted at the receiving end.

The results of the impedance measurements of the shorted 20-foot coaxial cable (Figure 13) showed the anticipated resonances.

The contractor also performed extensive measurements on a three-phase power distribution system associated with Radio Telegraph Transmitting Equipment Model TBK-17. This particular transmitter is capable of putting out 500 watts on c-w transmission from 2 to 18 megacycles. The impedance of the line (plus load) varied with frequency from 3000 ohms (maximum) to 30 ohms (minimum). Resonances, as indicated by points of high or low impedance, occurred at the same respective frequencies whether impedances were measured in a single phase or between two phases. For a single-phase measurement, both probes were connected around the same conductor and separated by only a small distance. For measurements between two phases, a probe was placed around each conductor of the two phases involved. This necessitated a large physical separation of the two probes. Impedances measured between two phases were about seven times those measured in one phase of the three-phase line due to the large separation of the current-probes.

The contractor performed numerous tests on the following noise-producing equipment:

1. A c-w interference source

2. An ac-dc rotary converter

3. A universal motor

From the values measured, the equivalent noise-source voltage and potential power output of the noise sources were calculated and correlated with presently used methods involving LISN. In addition, the amount of interference which would be conducted into a particular 60-cycle power-line connection was calculated and correlated with measured results. All measured and calculated values agreed closely, indicating this system of interference measurement was useful in measuring and predicting noise voltages.

It was found that measurement of impedance of the universal motor should be made only when the armature is spinning. Ideally, the test-sample motor shaft should be rotated by another motor at the rated speed of the test-sample motor. Preliminary measurements indicated however that the speed of shaft rotation is not important.

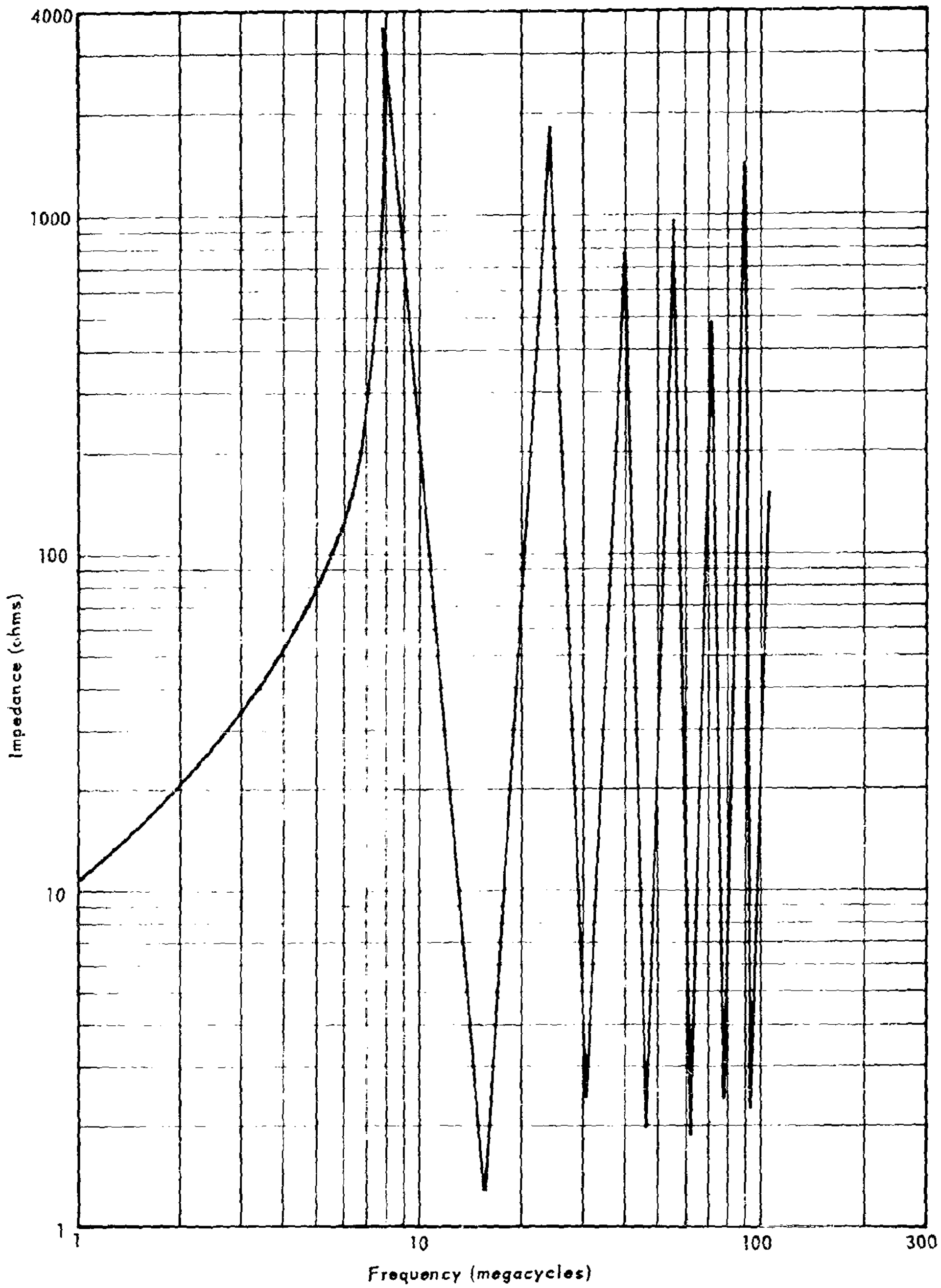

Figure 13. Curve of impedance measurements of shorted 20-foot coaxial cable (1 to 105 megacycles).

The contractor made the following general observations concerning his work and results.

It is very important to note that at present this is the only known method of measuring impedance in a closed-loop circuit where no connections must be broken. Examples of some practical applications of this would be antenna-impedance measurements while operating, and power-line-impedance measurements where large currents are flowing.

When measuring power-outlet RF impedances, care must be taken to insure that the signal generator and noise meter used are not plugged into the same line under test since this may alter the impedance being measured.

When test equipment did cause changes in the power-outlet impedance, it was usually the result of large filter capacitors connected across the power-line input to the equipment. Equipment that did not possess these capacitors only affected the line impedance slightly.

The impedances of normal power-line connections vary widely from a few ohms to several thousand ohms depending on the frequency of measurement, location of the point of measurement, line characteristics, and line terminations.

There will exist several resonances and anti-resonances on the average power line, the extent of which will depend upon the relationship of the factors just mentioned.

Although interference correlations and validity using the new techniques (on the test samples cited above) have been established, other types of test samples should be correlated. Examples of additional test samples are receivers, transmitters, diathermy equipment, and other electronic equipment.

Therefore it might be finally stated that the practical improvement limit and range of applications have not yet been ascertained.

CONTRACT WORK EVALUATION AND IMPROVEMENT AT NCEL

When the contract terminated in October 1960, the contractor submitted his final report and prototype instrument to this Laboratory. At that time a conference was held with the engineers who had worked on the project to discuss the possibilities of improving the measurement device. The principle improvement discussed was that of developing supporting instrumentation for the device to provide information about impedance phase angles in addition to the impedance magnitude already provided.

As a result of this conference it was determined that a study should be made by the Laboratory to determine the usefulness of information concerning the impedance phase angles by investigating the possible range of errors involved when phase information is not used.

This task was undertaken and the answer to the question concerning the usefulness of phase-angle information is presented in this report under Problem Analysis. The development of a method and circuitry for obtaining phase information has been accomplished and will be explained in the remainder of this report.

A method has been developed which permits the determination of the phase angle of the noise-source or load impedance utilizing the impedance setup previously described (Figure 8) in conjunction with a continuously variable-delay line and step attenuator. The setup is described in Figure 14.

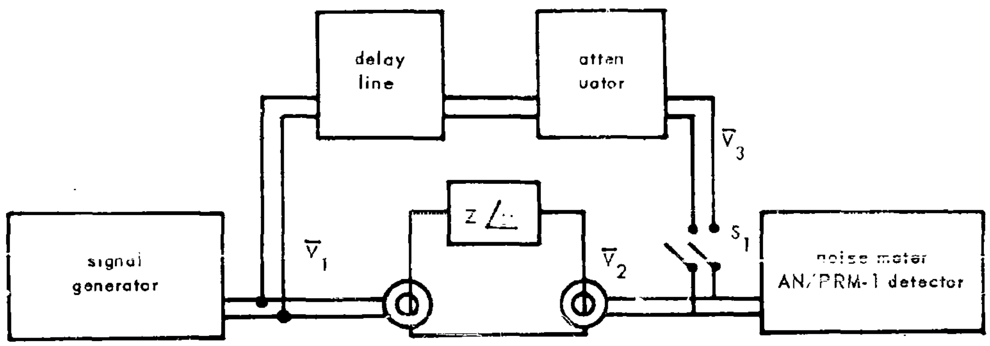

Figure 14. Measurement of both magnitude and phase of the unknown impedance ($Z \angle \theta$).

In this setup, the input signal is divided into two paths. The primary path is the normal impedance-magnitude-determination circuit. The second path is the comparison path. The magnitude of the impedance is determined in the same manner as before by reading $\overline{V}_1$ and $\overline{V}_2$ and calculating $\overline{Z}$. Then S_1 is closed, and the comparison path is adjusted until the voltage $\overline{V}_2 + \overline{V}_3 = 0$, indicated by a null on the noise meter. The delay-line time setting is read to obtain the total delay time at noise-meter null. This delay time is then compared to the time reading obtained using a pure resistance of the same magnitude as Z. The phase deviation is then calculated from the difference in the time readings (see Appendix C).

$$\Delta t = t - t_o$$

$$\theta = \frac{\Delta t}{T}(360) \qquad \text{where } T = \frac{1}{f}$$

or

$$\theta = \Delta t f(360) \tag{8}$$

With this technique the impedance of the noise source and load can be specified as to magnitude and phase angle. The noise voltage itself may be indirectly measured as previously explained. Once these quantities have been completely specified, it is possible to predict the noise voltage and power delivered by the noise source to any known load impedance.

Based on the above consideration, the contractor's current-probe impedance-measuring device was modified by the addition of the components outlined in the block diagram of Figure 14. A photograph of the device after modification is shown in Figure 15. The large double dial on the upper left is the control knob for the delay line and is calibrated in microseconds. It is this dial which is read for the time settings.

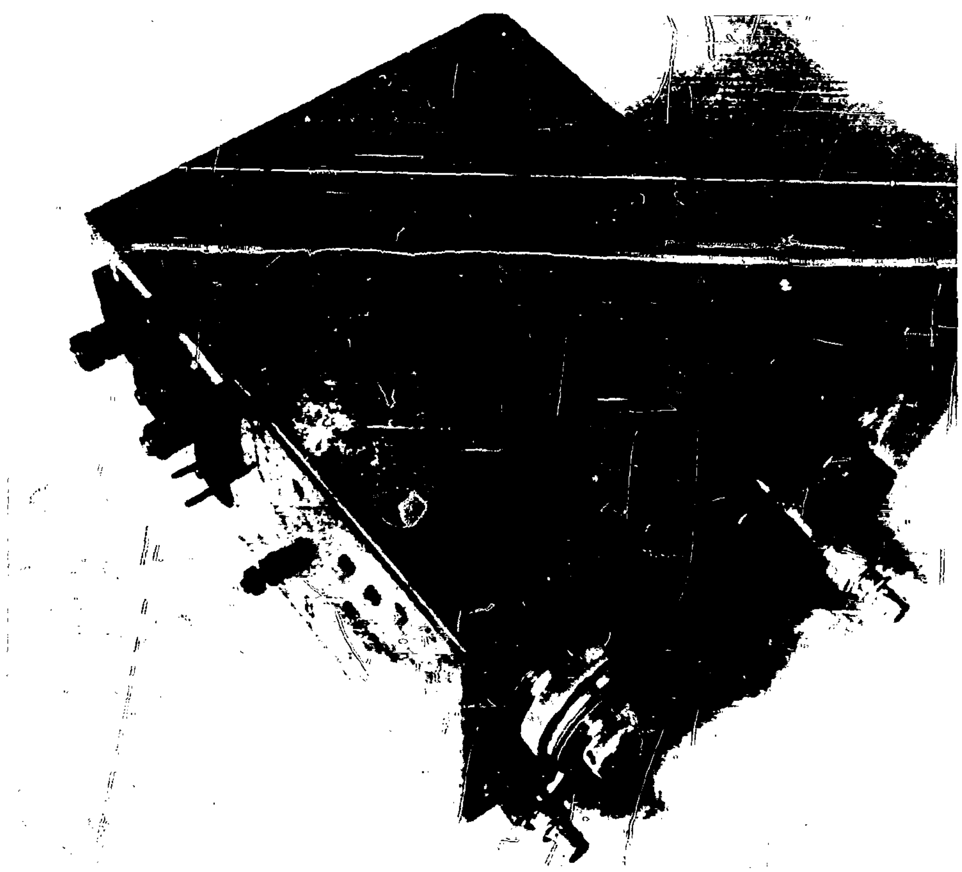

Figure 15. Modified impedance-measuring device.

The modified instrument now has the following performance features:

1. The impedance-magnitude-measuring capability is limited by current-probe transfer impedance which has a 3-db bandwidth of 0.5 to 45 megacycles.

2. The impedance-magnitude-measurement accuracy is within 20 percent when averaged K values are used in Equation 6, or better than 10 percent when a $\overline{V}_1/\overline{V}_2$ versus frequency nomograph is used in computations.

3. The phase-angle-measuring capability is limited from 2 megacycles to 30 megacycles. The lower-frequency limitation is due to the total delay of the delay line which is 0.5 microseconds. The higher-frequency limitation is due to poor response of the delay line above 30 megacycles.

4. The accuracy of the phase-angle measurements is ±20 percent from 2 to 30 megacycles for impedance magnitudes greater than 30 ohms. For impedance magnitudes less than 30 ohms the accuracy becomes progressively worse.

5. The power-current-carrying capability is 350 amps ac or dc

6. The instrument is constructed entirely of passive circuitry.

EXPERIMENTAL RESULTS OF IMPEDANCE-MAGNITUDE AND PHASE-ANGLE MEASUREMENTS

As a practical test of the ability of the device to measure phase angles, numerous frequency-dependent load impedances were inserted across the load terminals of the device and measured. These measured values were then plotted along with the impedance-bridge-measurement values of the loads. Two examples of the results of these tests are shown in Figures 16 and 17.

The next test performed on this device was to measure the source impedances of various electric motors. As indicated by the contractor's work, the impedance of anything which is connected by a length of line will vary with standing waves on the line, depending of course on the length of the line and frequency of measurement. An example of this is shown in Figure 18.

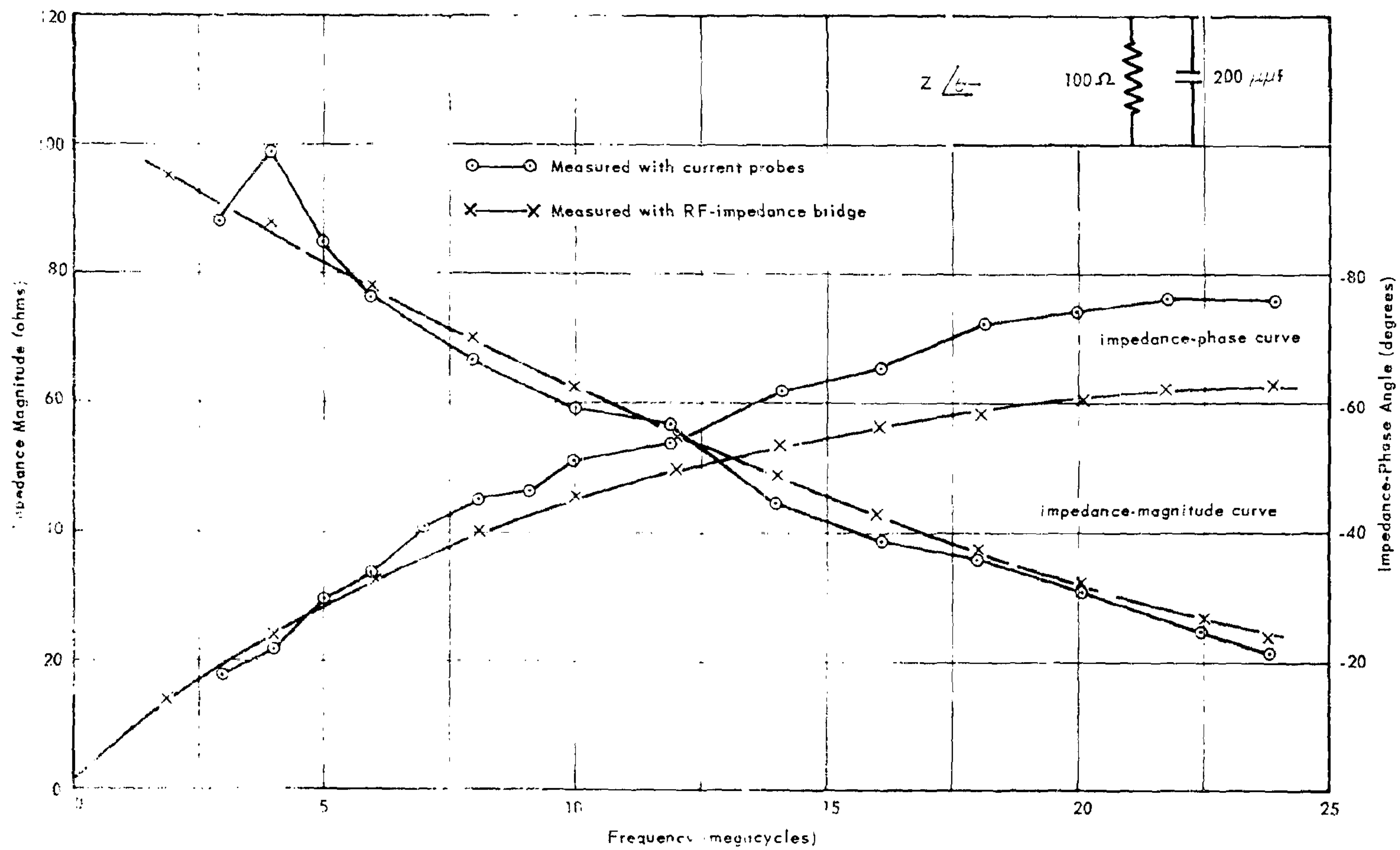

Figure 16. Measured impedance magnitude and phase versus frequency (RC network).

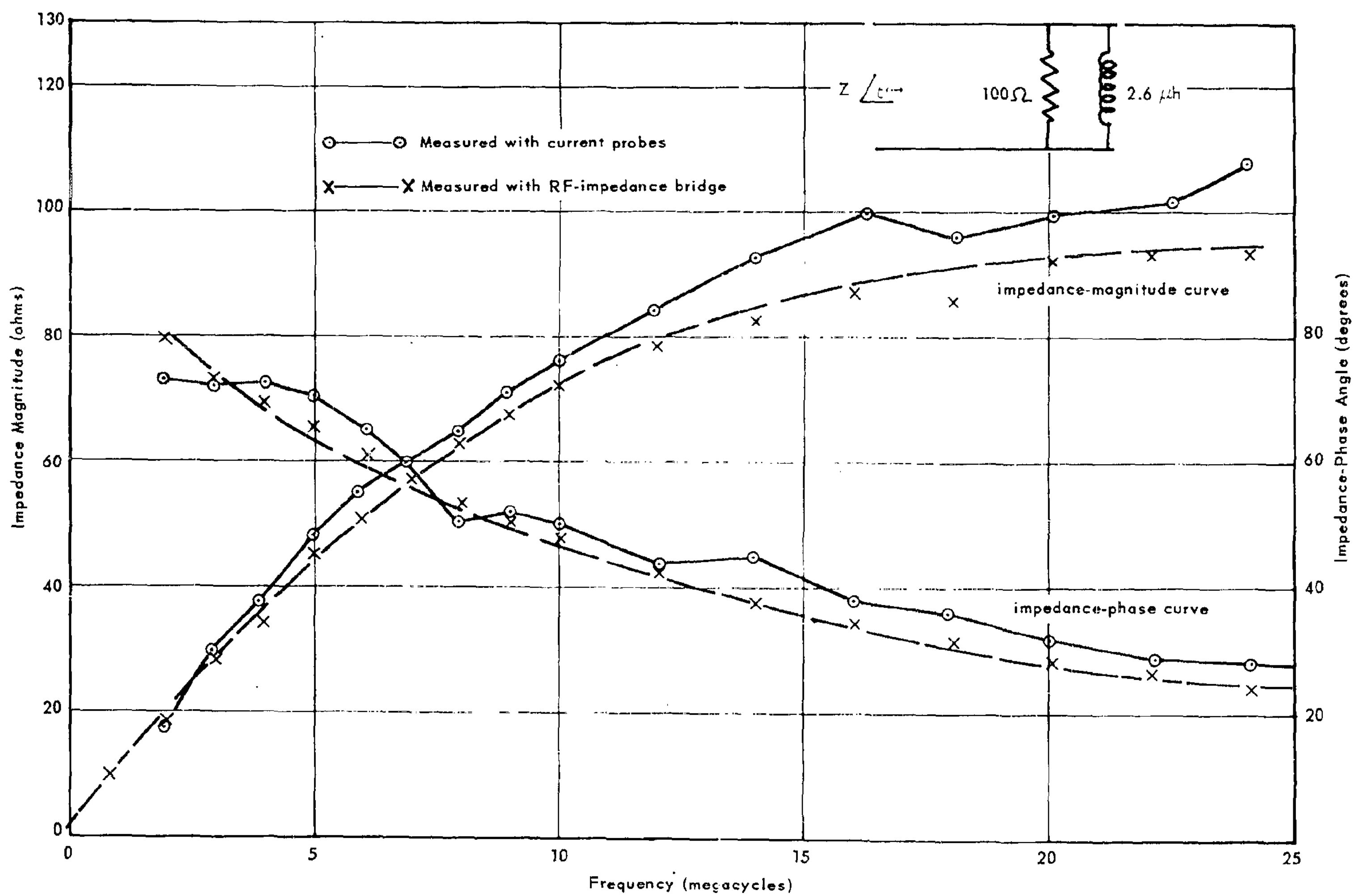

Figure 17. Measured-impedance magnitude and phase versus frequency (RL network).

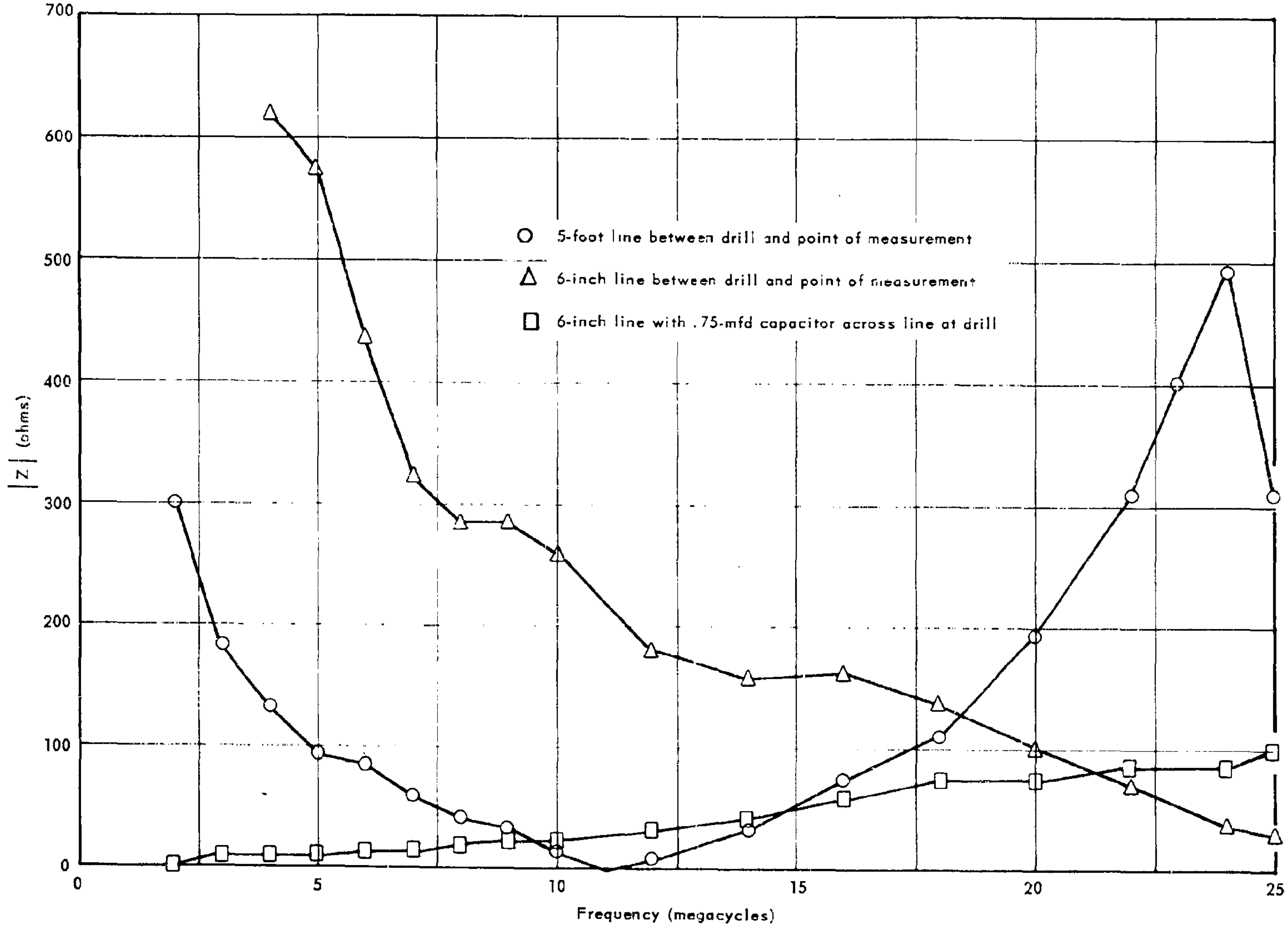

Figure 18. 3/4-inch-power-drill line-impedance characteristics.

An evaluation of the ability of the measurement system to predict the noise voltage from an arbitrary source across a known load impedance was performed by:

1. Measuring the equivalent noise-source impedance of a 3/4-inch electric power drill.

2. Measuring the equivalent noise-source short-circuit current.

3. Computing the equivalent noise-source voltage.

4. Computing the noise voltage which the noise-source equivalent circuit will present across a 50-ohm load.

5. Measuring the noise voltage that the power drill presented into a 50-ohm LISN load.

6. Comparing the computed value of noise voltage with the measured value. This test was run several times with satisfying results, an example of which is shown in Figure 19.

CONCLUSION

The two current-probe technique of measuring conducted radio-frequency interference has demonstrated a considerable superiority over the present method of measuring RFI with line-impedance-stabilization networks. The current-probe technique, though it is more time-consuming in operation, eliminates the ambiguities associated with conducted-noise measurements.

RECOMMENDATIONS

On the basis of the above conclusion, it is recommended that:

1. Further work be done to extend the useful frequency range of the instrument.

2. The two current-probe technique be incorporated into the Mil-I-16910A specification for measuring conducted RFI, in order to update and improve the conducted-RFI measurements being made in the Bureau of Ships and Bureau of Yards and Docks.

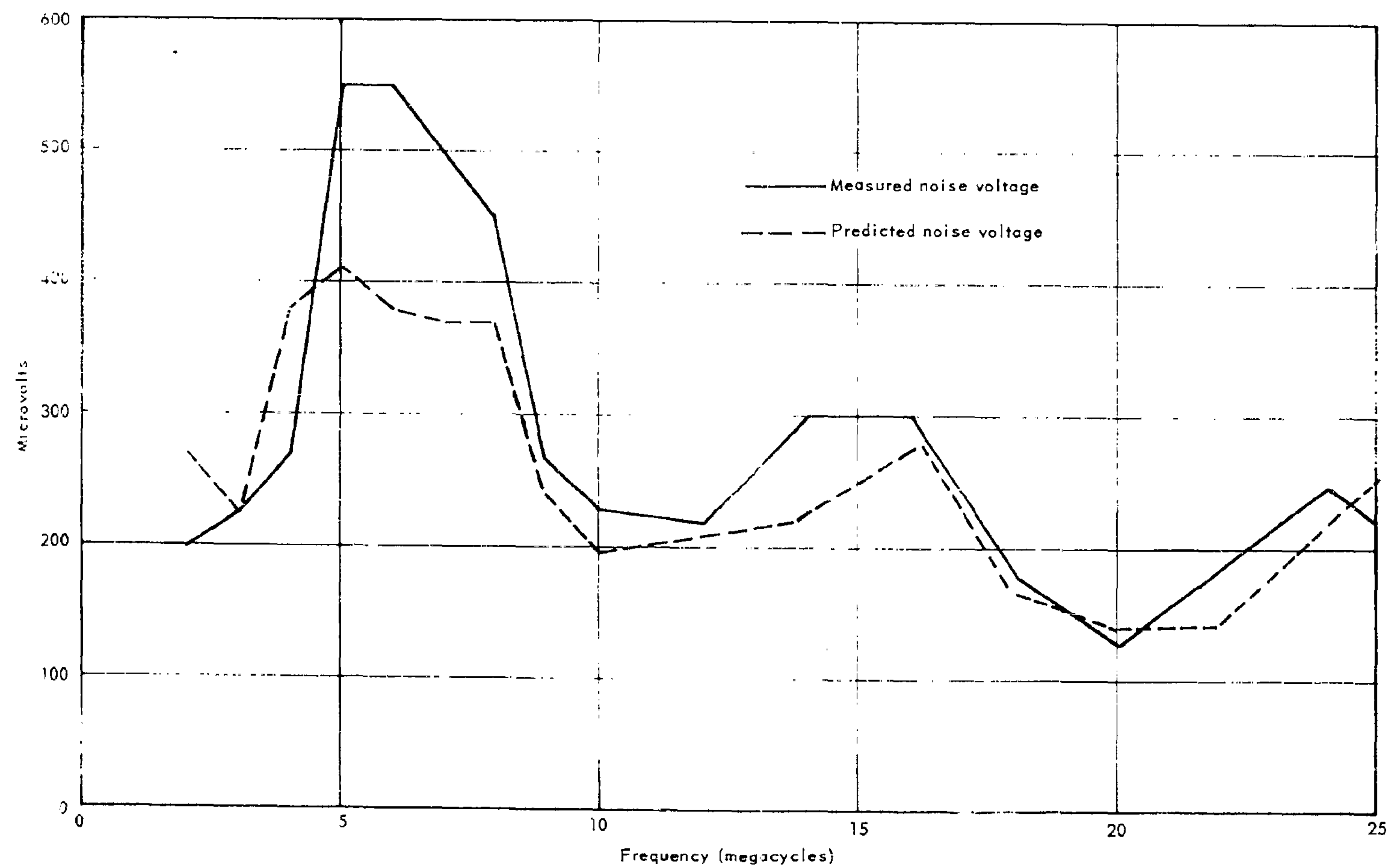

Figure 19. Conducted-noise voltage from 3/4-inch electric drill.

Appendix A

DERIVATION OF CURVES PRESENTED IN FIGURE 6

The ratio of the error voltage to the source voltage may be written as follows:

$$\frac{\bar{V}_{err}}{\bar{V}_s} = \frac{1}{1 + \frac{Z_s}{Z_L}} - \frac{1}{1 + \frac{Z_s}{R}}$$

Let

$$Z_1 \angle \theta_1 = \frac{Z_s}{Z_L}$$

and

$$Z_2 \angle \theta_2 = \frac{Z_s}{R}$$

Then

$$Z_1 \angle \theta_1 = |Z_1| (\cos\theta_1 + j \sin\theta_1)$$

and

$$Z_2 \angle \theta_2 = |Z_2| (\cos\theta_2 + j \sin\theta_2)$$

By substitution and expansion

$$\frac{\bar{V}_{err}}{\bar{V}_s} = \frac{1 + |Z_1| \cos\theta_1 - j|Z_1| \sin\theta_1}{1 + 2|Z_1| \cos\theta_1 + |Z_1^2|}$$

$$- \frac{1 + |Z_2| \cos\theta_2 - j|Z_2| \sin\theta_2}{1 + 2|Z_1| \cos\theta_2 + |Z_2^2|}$$

Now let
$$A = \frac{1 + |Z_1| \cos\theta_1}{1 + 2|Z_1| \cos\theta_1 + |Z_1^2|}$$

$$B = \frac{|Z_1| \sin\theta_1}{1 + 2|Z_1| \cos\theta_1 + |Z_1^2|}$$

$$C = \frac{1 + |Z_2| \cos\theta_2}{1 + 2|Z_2| \cos\theta_2 + |Z_2^2|}$$

$$D = \frac{|Z_2| \sin\theta_2}{1 + 2|Z_2| \cos\theta_2 + |Z_2^2|}$$

Then
$$\frac{\overline{V}_{err}}{\overline{V}_s} = (A - C) + j(D - B)$$

which may be written finally as:

$$\frac{\overline{V}_{err}}{\overline{V}_s} = \sqrt{(A - C)^2 + (D - B)^2}\ \angle \tan^{-1} \frac{(D - B)}{(A - C)}$$

Appendix B

DERIVATION OF EQUATION 6

The two current-probe method of measuring impedance may be represented as follows:

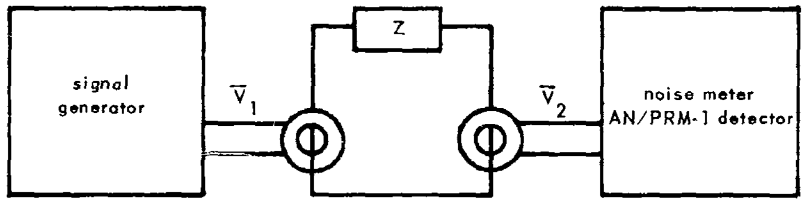

The equivalent circuit for this is:

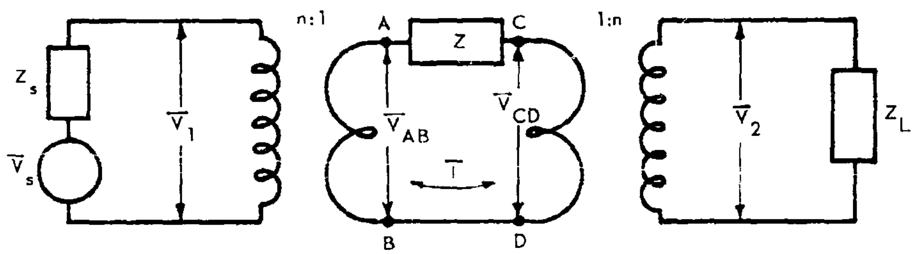

where Z_s = source impedance

$\bar{V}_s$ = source voltage

$\bar{V}_1$ = terminal voltage applied to input probe

$\bar{V}_2$ = terminal voltage across output probe

Z = unknown impedance

Z_L = detector input impedance

$\bar{I}$ = current induced into middle loop

$\bar{V}_{AB}$ = terminal voltage across secondary of first probe

$\bar{V}_{CD}$ = terminal voltage across primary of second probe

n = turns ratio of the current probes

Since the probes are identical and function in the circuit as transformers, the terminal-voltage relationships are:

$$\overline{V}_{AB} = \frac{\overline{V}_1}{n} \tag{B-1}$$

and

$$\overline{V}_{CD} = \frac{\overline{V}_2}{n} \tag{B-2}$$

The assumption will be made that the current-probes act as ideal transformers.

The impedance of the load (Z_L) will then be reflected into the middle loop as a load for $\overline{V}_{CD}$ as follows:

$$\overline{V}_{CD} = \overline{I}\left(\frac{Z_L}{n^2}\right) \tag{B-3}$$

The voltage relationships of the middle loop may now be written as:

$$\overline{V}_{AB} = \overline{I}Z + \overline{V}_{CD} \tag{B-4}$$

or, solving Equation B-3 for $\overline{I}$ and substituting,

$$\overline{V}_{AB} = \overline{V}_{CD}\left(n^2 \frac{Z}{Z_L} + 1\right) \tag{B-5}$$

Substituting $\overline{V}_1/n$ for $\overline{V}_{AB}$ and $\overline{V}_2/n$ for $\overline{V}_{CD}$ (as indicated by Equations B-1 and B-2) into Equation B-5,

$$\frac{\overline{V}_1}{n} = \frac{\overline{V}_2}{n}\left(n^2 \frac{Z}{Z_L} + 1\right) \tag{B-6}$$

Solving Equation B-6 for Z yields:

$$Z = \frac{Z_L}{n^2}\left(\frac{\overline{V}_1}{\overline{V}_2} - 1\right) \tag{B-7}$$

The quantity Z_L/n^2 by definition is a function of the detector and the probes used in the circuit. For any given situation this ratio will be constant and will be defined as:

$$K = \frac{Z_L}{n^2}$$

Unfortunately the detector used to measure V_1 and V_2 is only capable of measuring their magnitudes; therefore, Equation B-7 will be finally written as:

$$|Z| = K\left(\left|\frac{\overline{V}_1}{\overline{V}_2}\right| - 1\right) \tag{B-8}$$

Appendix C

DERIVATION OF EQUATION 8

In measuring the phase angle of the unknown impedance, the measuring system is shown in block diagram form:

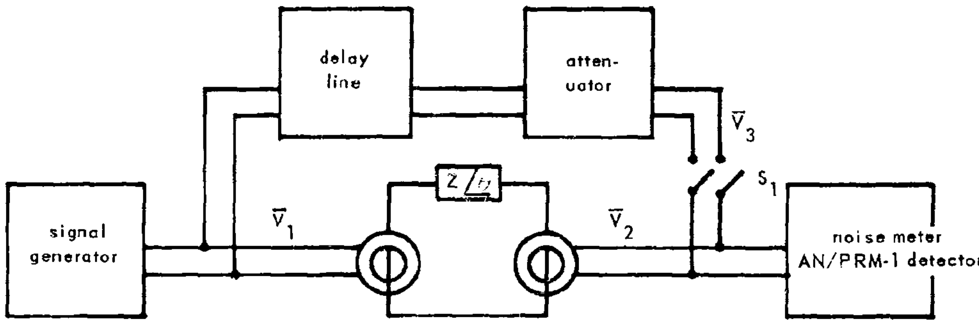

Figure 14. Measurement of both magnitude and phase of the unknown impedance ($Z\,\angle\theta$).

To measure the phase angle of the impedance (Z):

1. Measure the impedance magnitude $|Z|$ in the normal manner.

2. Close switch (S_1) and adjust both the delay line and attenuator simultaneously for a null on the detector.

3. Record the final time setting on the delay line as t_1.

4. Replace the impedance with a resistor of magnitude $R = |Z|$.

5. Readjust the delay line for a detector null. (The attenuator should not require readjusting.)

6. Record the new time setting on the delay line as t_2.

7. The phase angle θ of the impedance $Z\,\angle\theta$ is proportional to the time difference between t_1 and t_2 as indicated below.

$$\theta = (t_1 - t_2)(f)(360) \text{ degrees}$$

This equation may be derived as follows:

By rewriting equation B-8, the output voltage of the secondary current-probe is:

$$\bar{V}_2 = \bar{V}_1 \left(\frac{1}{1 + \frac{Z \angle \theta}{K}} \right)$$

Due to the inherent impedance of the particular circuitry used, it was found to be unreliable to use the comparison method for impedance magnitudes less than 30 ohms. Therefore the above equation will be simplified by making the following approximation:

If $$\frac{Z \angle \theta}{K} \gg 1$$

where $Z \angle \theta \geq 10$

$K \simeq 1$

Then $$\bar{V}_2 \simeq \bar{V}_1 \frac{K}{Z \angle \theta}$$

The voltage output of the comparison path circuit may be written as:

$$\bar{V}_3 = \bar{V}_1 A_1 \angle \varphi_1$$

where A_1 indicates magnitude and φ_1 indicates phase change. Then when the detector indicates a null output with Z as the load,

$$\bar{V}_2 + \bar{V}_3 = 0 \quad \text{or} \quad \bar{V}_2 = -\bar{V}_3 \quad \text{or} \quad A_1 \angle \varphi_1 = \frac{-K}{Z \angle \varphi} \qquad \text{(C-1)}$$

When the detector indicates a null output with the resistor $R = |Z|$ as a load,

$$A_2 \angle \varphi_2 = \frac{K}{R} \qquad \text{(C-2)}$$

Solving Equation C-2 for K and substituting this into Equation C-1 yields:

$$A_1 \angle \varphi_1 = \frac{1}{Z \angle \theta} (A_2 \angle \varphi_2) R$$

or

$$Z \angle \theta = R \frac{A_2 \angle \varphi_2}{A_1 \angle \varphi_1} = R \left(\frac{A_2}{A_1}\right) \angle \varphi_2 - \varphi_1$$

Since

$$R = |Z|$$

and

$$|A_2| = |A_1|$$

then

$$\theta = \varphi_2 - \varphi_1$$

where $\varphi_2 = \omega t_2$

$\varphi_1 = \omega t_1$

Then

$$\theta = 2\pi f (t_2 - t_1) \text{ radians} \qquad \text{(C-3)}$$

To obtain degrees, Equation C-3 may be rewritten as:

$$\theta = (t_2 - t_1)(f)(360)$$

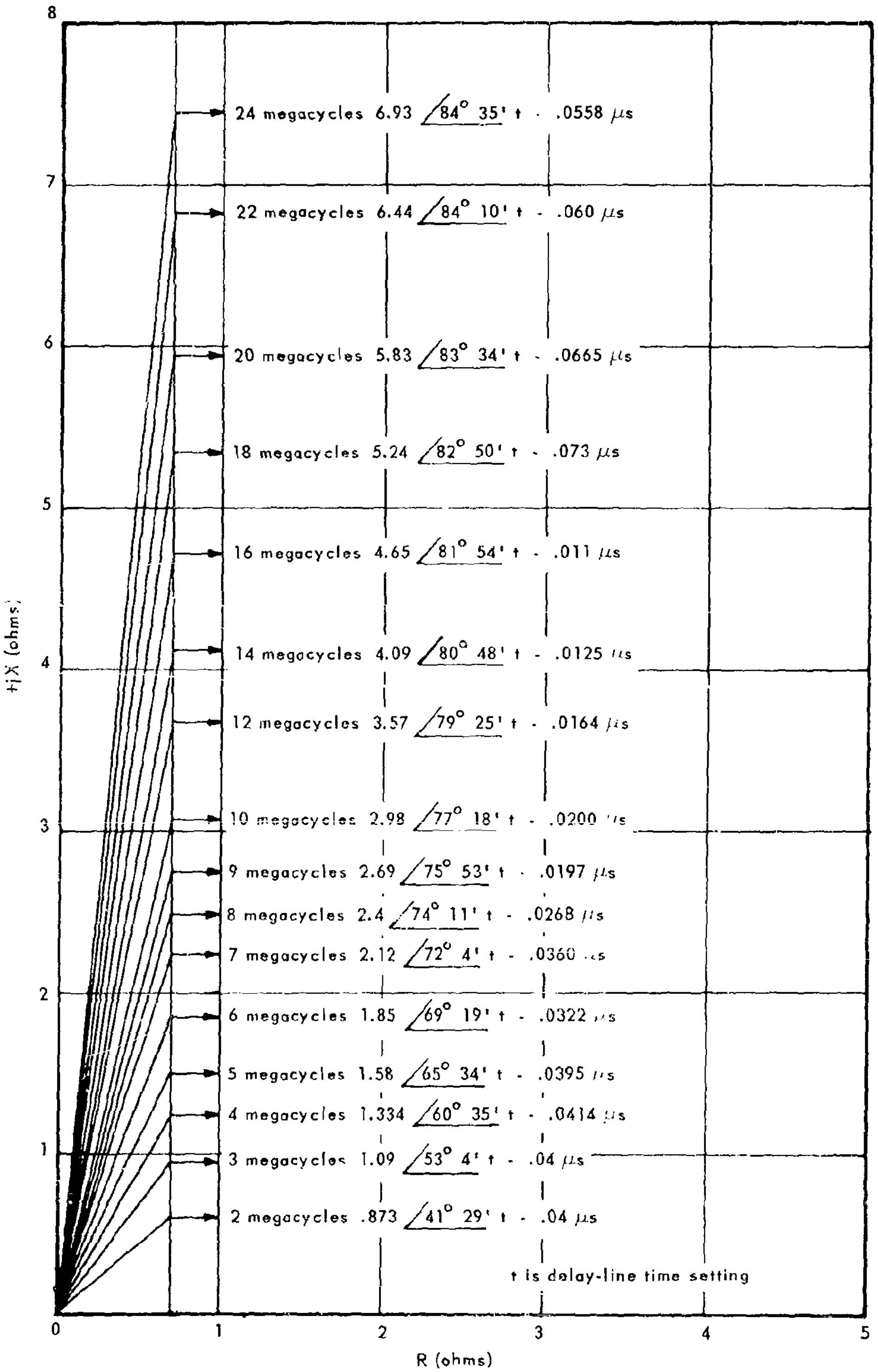

Figure 20. Internal-impedance magnitude and phase characteristics of measuring circuit.

To obtain the phase angle of an impedance less than 30 ohms a different technique must be used.

The problem arises from the fact that the coupling loop formed by the power-line shorting capacitor and load has an inherent impedance which may become as large as 10 ohms at the higher frequencies (see Figure 20). This impedance will be called Z_{loop} and must be corrected for in the following manner.

The time reading for the impedance of Z_{loop} is subtracted from the time reading of the impedance being measured. The angle between the two vectors is then calculated from this time reading:

$$\varphi = (t_1 - t_2)(f)(360) \qquad \text{(C-4)}$$

The two impedances are then drawn on a vector diagram:

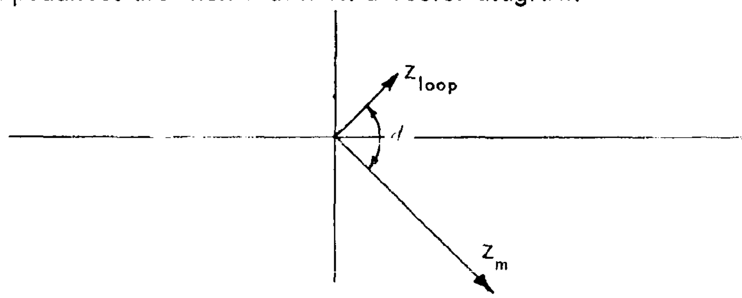

The correct value of the impedance and phase angle is now determined by obtaining the vector difference between Z_m and Z_{loop}:

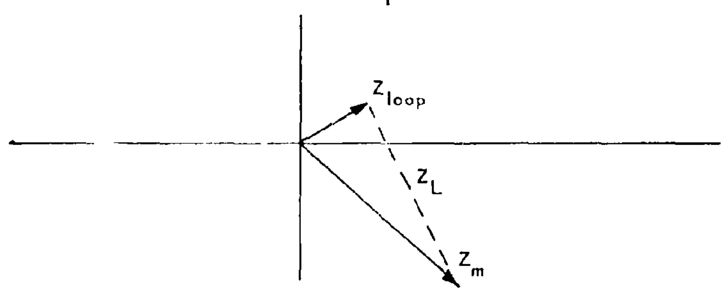

Fortunately, most of the commonly encountered impedances are greater than 30 ohms and this correction is not necessary. When resonance conditions are encountered with the resultant high- or low-impedance values, measurement at these resonant frequencies can be avoided. More accurate measurements at frequencies on either side of resonance can be made and the resonant impedances can be calculated.

DISTRIBUTION LIST

No. of copies	SNDL Code	
10		Chief, Bureau of Yards and Docks (Code 70)
1	23A	Naval Forces Commanders (Taiwan Only)
4	39B	Construction Battalions
10	39D	Mobile Construction Battalions
3	39E	Amphibious Construction Battalions
2	39F	Construction Battalion Base Units
1	A2A	Chief of Naval Research - Only
2	A3	Chief of Naval Operation (OP-07, OP-04)
5	A5	Bureaus
2	B3	Colleges
2	E4	Laboratory ONR (Washington, D. C. only)
1	E5	Research Office ONR (Pasadena only)
1	E16	Training Device Center
7	F9	Station - CNO (Boston; Key West; San Juan; Long Beach; San Diego; Treasure Island; and Rodman, C. Z. only)
6	F17	Communication Station (San Juan; San Francisco; Pearl Harbor; Adak, Alaska; and Guam only)
1	F21	Administration Command and Unit CNO (Saipan only)
1	F40	Communication Facility (Pt. Lyautey only)
1	F41	Security Station
1	F42	Radio Station (Oso and Cheltanham only)
1	F48	Security Group Activities (Winter Harbor only)
8	H3	Hospital (Chelsea; St. Albans, Portsmouth, Va; Beaufort; Great Lakes; San Diego; Oakland; and Camp Pendleton only)
1	H6	Medical Center
2	J1	Administration Command and Unit - BuPers (Great Lakes and San Diego only)
1	J3	U. S. Fleet Anti-Air Warfare Training Center (Virginia Beach only)
2	J4	Amphibious Bases
1	J19	Receiving Station (Brooklyn only)
1	J34	Station - BuPers (Washington, D. C. only)
1	J37	Training Center (Bainbridge only)
1	J46	Personnel Center
1	J48	Construction Training Unit
1	J60	School Academy
1	J65	School CEC Officers
1	J84	School Postgraduate
1	J90	School Supply Corps

Distribution List (Cont'd)

No. of copies	SNDL Code	
1	J95	School War College
1	J99	Communication Training Center
11	L1	Shipyards
4	L7	Laboratory - BuShips (New London; Panama City; Carderock; and Annapolis only)
5	L26	Naval Facilities - BuShips (Antigua; Turks Island; Barbados; San Salvador; and Eleuthera only)
1	L30	Submarine Base (Groton, Conn. only)
2	L32	Naval Support Activities (London & Naples only)
2	L42	Fleet Activities - BuShips
4	M27	Supply Center
7	M28	Supply Depot (Except Guantanamo Bay; Subic Bay; and Yokosuka)
2	M61	Aviation Supply Office
15	N1	BuDocks Director, Overseas Division
28	N2	Public Works Offices
7	N5	Construction Battalion Center
5	N6	Construction Officer-in-Charge
1	N7	Construction Resident-Officer-in-Charge
12	N9	Public Works Center
1	N14	Housing Activity
2	R9	Recruit Depots
2	R10	Supply Installations (Albany and Barstow only)
1	R20	Marine Corps Schools, Quantico
3	R64	Marine Corps Base
1	R66	Marine Corps Camp Detachment (Tengan only)
6	W1A1	Air Station
33	W1A2	Air Station
8	W1B	Air Station Auxiliary
4	W1C	Air Facility (Phoenix; Monterey; Oppama; Naha; and Naples only)
4	W1E	Marine Corps Air Station (Except Quantico)
1	W1F	Marine Corps Auxiliary Air Station
8	W1H	Station - BuWeps (Except Rota)
1		Deputy Chief of Staff, Research and Development, Headquarters, U. S. Marine Corps, Washington, D. C.
1		President, Marine Corps Equipment Board, Marine Corps School, Quantico, Va.
1		Mr. A. Goutos, Headquarters, European GEEIA (AFLC), United States Air Force, APO 332, New Yorl
1		Mr. F. W. Farr, Transmission Design Section, U. S. Department of the Interior, Bonneville Power Administration, Portland, Ore.

No. of copies	
1	Chief of Staff, U. S. Army, Chief of Research and Development, Department of the Army, Washington, D. C.
1	*Office of the Chief of Engineers, Assistant Chief of Engineering for Civil Works, Department of* the Army, Washington, D. C.
1	Chief of Engineers, Department of the Army, Attn: Engineering R & D Division, Washington, D. C.
1	Chief of Engineers, Department of the Army, Attn: ENGCW-OE, Washington, D. C.
1	Director, U. S. Army Engineer Research and Development Laboratories, Attn: Information Resources Branch, Fort Belvoir, Va.
1	Headquarters, Wright Air Development Division, (WWAD-Library), Wright-Patterson Air Force Base, Ohio
3	Headquarters, U. S. Air Force, Directorate of Civil Engineering, Attn: AFOCE-ES, Washington, D. C.
1	Commanding Officer, U. S. Navy Yards and Docks Supply Office, U. S. Naval Construction Battalion Center, Port Hueneme, Calif.
1	*Deputy Chief of Staff, Development, Director of Research and Development, Department of the* Air Force, Washington, D. C.
1	Director, National Bureau of Standards, Department of Commerce, Connecticut Avenue, Washington, D. C.
2	Office of the Director, U. S. Coast and Geodetic Survey, Washington, D. C.
10	Armed Services Technical Information Agency, Arlington Hall Station, Arlington, Va.
2	Director of Defense Research and Engineering, Department of Defense, Washington, D. C.
2	Director, Division of Plans and Policies, Headquarters, U. S. Marine Corps, Washington, D. C.
2	Director, Bureau of Reclamation, Washington, D. C.
1	Facilities Officer (Code 108), Office of Naval Research, Washington, D. C.
1	Commanding Officer, U. S. Navy Construction Battalion Center, Port Hueneme, Calif., *Attn: Materiel Department (Code 140)*
2	Mr. Stanton Bennett, Officer in Charge of Construction, 1156 15th Street, N. W., Room 313, Washington, D. C.
2	Bureau of Ships (Code 695-B), Department of the Navy, Washington, D. C.
1	Mr. Guy Johnson, Communications Department, U. S. Army Signal Research Dev. Lab., Fort Monmouth, N. J.
1	Mr. J. Fred Chappel, Communications Department, U. S. Army Signal Research Dev. Lab., Fort Monmouth, N. J.
1	Electronics Branch, Material Laboratory, U. S. Naval Shipyard, Brooklyn
1	Aeronautical Electronic & Electrical Laboratory, *Naval Air Development Center, Johnsville, Pa.*
1	Headquarters, U. S. Air Force Security Service, San Antonio, Tex., Attn: Asst. Dir. Maintenance & Plant Engineering, DCS/Communications-Electronics (ESD)
5	Commanding Officer and Director, U. S. Army Electronic Proving Ground, Fort Huachuca, Ariz., Attn: W. R. Foley
1	Mr. Harold C. Hurlbut, Department of the Navy, Northwest and Alaskan Division, Bureau of Yards and Docks, 1638 West Lawton Way, Seattle, Wash.

Distribution List (Cont'd)

No. of Copies	
1	Commandant, Industrial College of the Armed Forces, Washington, D. C.
1	Commandant, U. S. Armed Forces Staff College, U. S. Naval Base, Norfolk, Va.
1	Chief, Bureau of Ships, Attn: Chief of Research and Development Division, Navy Department, Washington, D. C.
1	Officer in Charge, U. S. Navy Unit, Rennselaer Polytechnic Institute, Troy, N. Y.
1	Chief, Bureau of Naval Weapons, Attn: Research Division, Navy Department, Washington, D. C.
1	Commander, Pacific Missile Range, Attn: Technical Director, Point Mugu, Calif.
1	Officer in Charge, U. S. Naval Supply Research and Development Facility, Naval Supply Center, Bayonne, N. J.
1	Commander, U. S. Naval Shipyard, Attn: Material Laboratory, Brooklyn, N. Y.
1	Office of Naval Research Branch Office, Navy No. 100, Box 39, FPO, New York
1	Commanding Officer, Naval Electronics Laboratory, Attn: Technical Director, San Diego
1	Commanding Officer, Fleet Training Center, Navy No. 128, c/o FPO, San Francisco
1	Deputy Chief of Staff, Research & Development Headquarters, U. S. Marine Corps, Washington, D. C.
1	Chief of Ordnance, U. S. Army, Attn: Research & Development Laboratory, Washington, D. C.
1	U. S. Army, Attn: Director of Research and Development Group, Washington, D. C.
1	President, Signal Corps Board, U. S. Army, Fort Monmouth, N. J.
1	Commanding Officer, Signal Corps Engineering Labs., Fort Monmouth, N. J.
1	U. S. Army Corps of Engineers, Office of the District Engineer, St. Paul District, 1217 U.S.P.O. and Customs House, St. Paul, Minn.
1	Coles Signal Laboratory, Red Bank, N. J.
1	Air Force Cambridge Research Center, Hanscom Field, Bedford, Mass.
1	Commander, Air Research & Development Command, Attn: Library, Andrews Air Force Base, Washington, D. C.
1	Directorate of Research, Air Force Special Weapons Center, Kirtland Air Force Base, N. M.
1	Sandia Corporation, Attn: Classified Document Division, Box 5800, Albuquerque, N. M.
1	Chief, Physical Research Branch, Research Division, U. S. Department of Commerce, Bureau of Public Roads, Washington, D. C.
1	HQ Western GEEIA Region, McClellan Air Force Base, Sacramento, Calif., Attn: Z.S.M.E.G.
2	Deputy Director, Air Force, Electronic Compatibility & Analysis Center, Naval Engineering Experiment Station, Annapolis, Md.
2	Deputy Director, Navy, Electronic Compatibility & Analysis Center, Naval Engineering Experiment Station, Annapolis, Md.

U. S. Naval Civil Engineering Laboratory.
Technical Report R-214.
THE TWO CURRENT-PROBE METHOD OF MEASURING CONDUCTED RADIO-FREQUENCY INTERFERENCE, by James L. Brooks.
37 p. illus. 28 Sept 62 OFFICIAL USE ONLY

An evaluation of a device to measure conducted interference. Both noise-source impedance and load impedance may be obtained.

1. Radio Frequency Interference, two current-probe method of measuring
I. Brooks, J. L.
II. Y-F006-09-205

U. S. Naval Civil Engineering Laboratory.
Technical Report R-214.
THE TWO CURRENT-PROBE METHOD OF MEASURING CONDUCTED RADIO-FREQUENCY INTERFERENCE, by James L. Brooks.
37 p. illus. 28 Sept 62 OFFICIAL USE ONLY

An evaluation of a device to measure conducted interference. Both noise-source impedance and load impedance may be obtained.

1. Radio Frequency Interference, two current-probe method of measuring
I. Brooks, J. L.
II. Y-F006-09-205

U. S. Naval Civil Engineering Laboratory.
Technical Report R-214.
THE TWO CURRENT-PROBE METHOD OF MEASURING CONDUCTED RADIO-FREQUENCY INTERFERENCE, by James L. Brooks.
37 p. illus. 28 Sept 62 OFFICIAL USE ONLY

An evaluation of a device to measure conducted interference. Both noise-source impedance and load impedance may be obtained.

1. Radio Frequency Interference, two current-probe method of measuring
I. Brooks, J. L.
II. Y-F006-09-205

U. S. Naval Civil Engineering Laboratory.
Technical Report R-214.
THE TWO CURRENT-PROBE METHOD OF MEASURING CONDUCTED RADIO-FREQUENCY INTERFERENCE, by James L. Brooks.
37 p. illus. 28 Sept 62 OFFICIAL USE ONLY

An evaluation of a device to measure conducted interference. Both noise-source impedance and load impedance may be obtained.

1. Radio Frequency Interference, two current-probe method of measuring
I. Brooks, J. L.
II. Y-F006-09-205